The Rates of S_N2 Reactions and Their Relation to Molecular and Solvent Properties

Luis G. Arnaut* and Sebastião J. Formosinho[a]

Abstract: The energy barriers of symmetrical methyl exchanges in the gas phase have been calculated with the reaction path of the intersecting/interacting-state model (ISM). Reactive bond lengths increase down a column of the Periodic Table and compensate for the decrease in the force constants, which explains the near constancy of the intrinsic barriers in the following series of nucleophiles: $F^- \approx Cl^- \approx Br^- \approx I^-$. This compensation is absent along the rows of the Periodic Table and the trend in the reactivity is dominated by the increase in the electrophilicity index of the nucleophile in the series $C < N < O < F$. Solvent effects have been quantitatively incorporated into the ISM model throu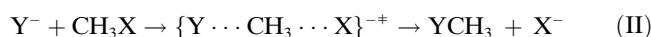gh a correlation between electrophilicity and the solvent acceptor number. This correlation is transferable between nucleophiles and solvents and allows the methyl transfer rate constants in solution to be calculated with remarkable simplicity and accuracy. The relationship between the S_N2 and electron-transfer mechanisms is clarified and it is shown that smaller solvent static effects should be expected for electron transfer in the absence of a thermodynamic driving force.

Keywords: electron transfer · nucleophilic substitution · rate constants · solvent effects · structure-activity relationships

Introduction

A substitution reaction is characterised by the replacement of a molecule (or ion) from the coordination shell of a reactive centre by another molecule (or ion) from the reaction medium, irrespective of whether it is a gas or a liquid. During the substitution the bond between the ligand and the reactive centre is broken, while a new bond is formed between that centre and the new species entering the coordination shell. When the electron pair accompanies the leaving group X, it is called nucleophilic substitution [Mechanism (I), in which Y^- is the nucleophilic reagent]. The current classification of aliphatic nucleophilic substitutions is based on the molecularity of their rate-determining step and distinguishes between first-order (S_N1) and second-order (S_N2) nucleophilic substitutions.[1] Textbooks often present S_N2 and S_N1 reactions as the example of two extremes of a mechanistic continuum.[2–4] Owing to the high ionisation potential of the $CH_3^\cdot$ radical, methyl group transfers are classed as S_N2 substitution reactions. Its molecularity is related to highly synchronised bond-breaking and -making events in the transition state [Mechanism (II)].

$$Y{:}^- + R{:}X \rightarrow Y{:}R + X{:}^- \tag{I}$$

$$Y^- + CH_3X \rightarrow \{Y \cdots CH_3 \cdots X\}^{-\ddagger} \rightarrow YCH_3 + X^- \tag{II}$$

The history of S_N2 reactions closely parallels the development of concepts such as structure–reactivity relationships, linear free-energy relationships, steric inhibition, kinetics as a probe of mechanism, stereochemistry as a probe of mechanism and solvent effects, and places them among the most fundamental processes in chemistry.
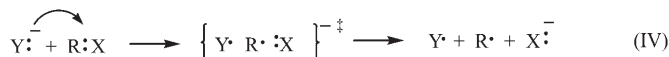
The relationship between S_N2 and electron-transfer (ET) reaction mechanisms has also been intensively explored. The S_N2 and ET reactions [Mechanisms (I) and (III)] can be represented on the same potential-energy surface following the observation that the net effect of S_N2 reactions is the transfer of a single electron from the nucleophile to the leaving group.[5,6]

$$Y{:}^- + R{:}X \rightarrow Y^\cdot + R^\cdot + X{:}^- \tag{III}$$

[a] Prof. L. G. Arnaut, Prof. S. J. Formosinho
Chemistry Department
University of Coimbra
P-3049 Coimbra Codex (Portugal)
Fax: (+351) 239-827703
E-mail: lgarnaut@ci.uc.pt

Note that the dimerisation of the radicals Y· and R· leads to products that are indistinguishable from the products of Mechanism (I), and that this process can be very fast in a solvent cage. Mechanism (IV) is an outer-sphere ET from the point of view of the electron donor and an inner-sphere ET from the point of view of the electron acceptor.[7]

$$Y\colon^- + R\colon X \longrightarrow \left[Y\cdot \ R\cdot \ \colon X \right]^{-\ddagger} \longrightarrow Y\cdot + R\cdot + X\colon^- \qquad (IV)$$

There are at least three different views on the relationship between S_N2 and ET reactions: 1) S_N2 and outer-sphere ET reactions are extremes of a spectrum of different transition states, with the inner-sphere ET in between.[7–10] 2) They occur on the same potential energy surface, but along different reaction coordinates and are competitive.[11–13] 3) They are served by the same transition state, the S_N2 and ET products branching out as the reactive trajectories descend from the transition state.[14–16] It is remarkable that the relationship between S_N2 and ET reactions continues to provide stimulating ideas about reactivity and mechanism in organic chemistry, even though they are among the most widely studied chemical reactions.

A conceptual understanding of the energy variations along the reaction coordinate of S_N2 reactions was provided by the model of Shaik and Pross and is based on valence-bond (VB) theory.[17,18] The key feature of this model is the representation of the reactants and products by VB wave-functions and the recognition that they are incorporated into well-defined excited states of products and reactants. In the simplest approximation of this VB theory, and for the case of symmetrical exchanges (Y=X), only three VB structures are considered, one representing the reactants ($X\colon^-$ $CH_3\cdot^-·X$), another the transition state ($X\colon^-$ CH_3^+ $^-\colon X$) and

Abstract in Portuguese: *O caminho de reacção do Modelo de Intersecção/Interacção de Estados (ISM) é usado para calcular as barreiras de energia de trocas simétricas de grupos metilo em fase gasosa. O aumento dos comprimentos das ligações reactivas ao longo de um grupo da Tabela Periódica compensa a correspondente diminuição das constantes de força e explica a quase constância das barreiras intrínsecas na série de nucleófilos $F^- \approx Cl^- \approx Br^- \approx I^-$. Esta compensação não ocorre ao longo de um período e o padrão de reactividade é dominado pelo aumento do índice de electrofilicidade do nucleófilo no período $C < N < O < F$. Os efeitos de solvente são quantitativamente incorporados no ISM usando uma correlação entre electrofilicidade e o número aceitador do solvente. Esta correlação é transferível entre nucleófilos e solventes, e permite calcular as constantes de velocidade de transferência de metilos em solução com notáveis simplicidade e rigor. Clarifica-se a relação entre mecanismos S_N2 e de transferência de electrão, e mostra-se que, para reacções atérmicas, são esperados menores efeitos estáticos de solvente para as transferências de electrão.*

the last one the products ($X\cdot^-·CH_3$ $^-\colon X$). The barrier of the reaction is expressed as a fraction (f) of the vertical electron-transfer energy from $X\colon^-$ to CH_3X, from which the avoided crossing interaction (B) is subtracted, [Eq. (1), in which I_P and E_A are the ionisation potential and electron affinity, respectively]. The activation energy reflects the size of the vertical electron-transfer energy and the resistance to molecular distortions, with this latter parameter reflected by the value of f. The value of the curvature factor f depends on the energy curve employed to derive Equation (1).

$$\Delta E^\ddagger = f[I_P(X\colon^-) - E_A(CH_3X)] - B \qquad (1)$$

For example, when two identical parabolae are employed, then $f = 0.25$ and a Marcusian-type expression is obtained in which the energy gap $I_P(Y\colon) - E_A(RX)$ replaces the reorganisation energy λ in the Marcus expression. The avoided crossing interaction, which is the resonance in the transition state, has been related to the degree of positive charge on the CH_3 group and to the bond dissociation energy of the C–X bond.[19]

Although the VB model provides important insights into S_N2 reactivity, most of the current theoretical investigations of gas-phase S_N2 reactions rely on high-level ab initio molecular-orbital calculations because they provide accurate reaction barriers.[20–28] Particularly enlightening are the systematic calculations of Hoz and co-workers,[27] which showed the internal barriers of gas-phase symmetrical methyl group transfers increase from right to left across the Periodic Table, but remain approximately constant down the column of the nucleophilic atom X. These unexpected reactivity trends have been interpreted in terms of a very simple formulation of the intersecting-state model[29] and further explored through the study of S_N2 reactions on nitrogen.[30]

We recently refined the intersecting-state model to quantitatively express the interactions between the intersecting states in terms of the properties of reactants and products.[31] The improved version of the intersecting/interacting-state model (ISM) proved valuable in calculations of absolute rate constants of atom and proton transfer reactions.[31–33] This work takes advantage of such refinements to relate the barriers of methyl transfers to the properties of the reactants and products. Additionally, we present a very simple but quantitative approach to the analysis of effects of solvent on the reaction rates.

Theory and Methodology

The first step of the ISM involves determining the lengths of the reactive bonds in the transition state. Then, in the second step, a function describing the energy difference between the equilibrium and transition-state configurations is employed to calculate the energy barrier. For a symmetrical methyl transfer reaction, the first step is simply the calculation of the X···CH_3 bond length in the transition state. By using the assumption of bond order conservation of the BEBO model[34] and Pauling's relationship between bond order and bond length,[35] the bond extension from equilibrium (l_{XC}) to the transition state ($l_{XC}^\ddagger$) is expressed by Equa-

tion (2), in which a is a constant and n^+ is the bond order in the transition state.

$$l_{XC}{}^+ - l_{XC} = -a\ln(n^+) \qquad (2)$$

Earlier applications of the ISM to atom and proton transfers showed that the proportionality between bond extensions and the logarithm of the bond order has a greater generality when it is applied to the equilibrium bond lengths of both reactants and products [Eq. (3), in which $a' = 0.182$]. This expresses the fact that longer bonds tend to distort more than shorter ones and that two bonds are present in the transition state. In the specific case of symmetrical methyl transfers ($l_{XC} = l_{YC}$), for which the transition-state bond order is $n^+ = 0.5$, then the bond extension is given by Equation (4).

$$l_{XC}{}^+ - l_{XC} = -a'(l_{XC} + l_{YC})\ln(n^+) \qquad (3)$$

$$l_{XC}{}^+ - l_{XC} = -2a'l_{XC}\ln(0.5) \qquad (4)$$

Earlier applications of the ISM employed either harmonic oscillators or Morse curves. Naturally, the value of the scaling factor a' will depend on the potential energy function employed to describe the extension of the reactive bond from equilibrium to the transition-state configuration. In this study of methyl transfers we calculated the transition-state bond extensions ($l_{XC}{}^+$) and energies (ΔV^+) by using both Morse curves (the data for the relevant C−X bonds are given in Table 1) and harmonic oscillators. The harmonic force constant can be obtained from Morse curve data by using Equation (5); the depth of the potential minimum, D_e, employed in the Morse curves is calculated from the bond dissociation energies determined at 298 K ($D_{298}{}^\ominus$) by using the correction for the bond strengths at absolute zero and the correction for the zero-point energies, $D_e = D_{298}{}^\ominus - 1.5RT + 0.5hc\omega_e$.[31]

$$f_{XC} = 2D_e\beta^2 \qquad (5)$$

The spectroscopic constant β is related to the electronic dissociation energy of the X−CH$_3$ bond, the equilibrium stretching frequency (ω_e) and the reduced mass (μ) through Equation (6), in which $\omega_e = \tilde{\nu} + 0.5hc\tilde{\nu}^2/(D_{298}{}^\ominus - 1.5RT)$ and $\tilde{\nu}$ is the observed infrared stretching frequency.[43] Morse curves require a higher scaling factor a' to give comparable values of $l_{XC}{}^+$ and ΔV^+. In view of the simple relationship between molecular structure and chemical reactivity pursued in this work and of the similarity between appropriately scaled calculations with Morse curves or harmonic oscillators, in this work we will focus on the use of harmonic oscillators.

$$\beta = \omega_e\sqrt{\frac{2\pi^2c\mu}{hD_e}} \qquad (6)$$

The transition-state bond lengths given by Equation (4) with $a' = 0.182$ are compared in Figure 1 with the corresponding values obtained by high-level ab initio calculations for symmetrical methyl transfers, in
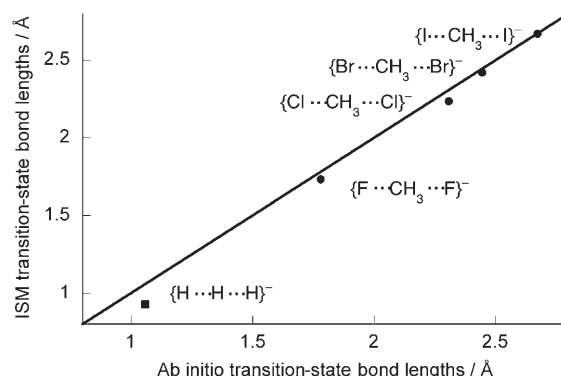

Figure 1. Comparison between the ISM and ab initio transition-state bond lengths of symmetrical methyl exchanges in the gas phase (●) and of H$^-$ + H$_2$ exchange (■). The ab initio data were taken from refs. [28, 20, 42]. The line is the ideal correlation. See the Supporting Information for details.

which X = F, Cl, Br or I.[20,28] There is a good agreement between ISM and ab initio calculations. We do not assign a special meaning to the fact that the scaling factor previously employed for atom and proton transfers also works for S$_N$2 reactions, but it is a remarkable achievement that Equation (3) provides meaningful transition-state bond lengths for such diverse reactions with such a simple scaling factor.

Hydrogen atom and proton transfers have significant tunnelling corrections and their rates can only be calculated when the full reaction path is accurately known. However, tunnelling of methyl groups is negligible at room temperature and so we do not have to calculate the full reaction path to obtain kinetically relevant results. Thus, we can explore the kinetics of symmetrical methyl transfers with the bond extensions given by Equation (4) and harmonic oscillators for the X−CH$_3$ bond extensions. The energy barrier for a symmetrical methyl transfer is then given by Equation (7), in which m is Parr's electrophilicity index.[44] The electrophilicity index gives the saturation point for electron inflow at the transition state, at which it attains a value given by Equation (8).

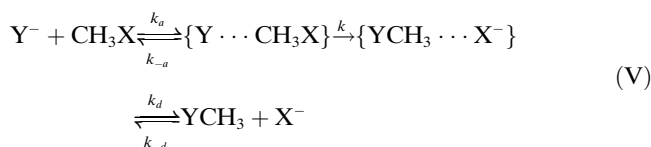$$\Delta V^+ = \frac{1}{2}\frac{f_{CX}}{m^2}[-2l_{CX}\ln(0.5)a']^2 \qquad (7)$$

$$m = \frac{I_p + E_A}{I_p - E_A} \qquad (8)$$

Table 1. Bond lengths, bond dissociation energies, vibrational frequencies, harmonic force constants of the molecules and ionisation potentials and electron affinities of the radicals employed in the calculation of the energy barriers of H-atom and methyl transfer reactions.

	l_{eq}[a] [Å]	$D_{298}{}^\ominus$[a] [kcal mol^{-1}]	$\tilde{\nu}$ [cm^{-1}]	f [kcal mol^{-1} Å^{-2}]	I_p[b] [eV]	E_a[b] [eV]
H−H	0.7414	104.2[a]	4161[c]	821	13.598	0.75419
CH$_3$−H	1.087	104.9[a]	2917[d]	720	9.843	0.08
CH$_3$CH$_2$−CH$_3$	1.532	88.5[e]	1054[d]	585	8.117	−0.26
CH$_3$NH−CH$_3$	1.455	82.2[b]	1079[d]	662	6.7	0.504
CH$_3$O−CH$_3$	1.416	82.9[f]	1102[b]	732	10.720	1.57
HO−CH$_3$	1.4246	92.1[g]	1033[d]	640	13.017	1.8277
F−CH$_3$	1.382	115.0[g]	1049[d]	704	17.423	3.448
CH$_3$S−CH$_3$	1.807	73.6[a]	743[d]	420	9.262	1.867
Cl−CH$_3$	1.785	83.7[b]	732[d]	416	12.968	3.6144
Br−CH$_3$	1.933	72.1[b]	611[d]	340	11.814	3.3636
I−CH$_3$	2.132	57.6[b]	533[h]	271	10.451	3.0590

[a] See ref. [36]. [b] From http://webbook.nist.gov/. [c] Observed frequency, see ref. [37]. [d] From the experimental frequency in http://srdata.nist.gov/cccbdb/. [e] See ref. [38]. [f] From the enthalpies of formation in ref. [39]. [g] See ref. [40]. [h] See ref. [41].

The function describing the change of m from unity in the reactant's X–C bond to the value given by Equation (8) for the transition state has been discussed in detail elsewhere,[33] but it is not relevant for this study because it does not require the full reaction path. Our interest is in the energy of the transition state and this is simply given by Equations (7) and (8) for symmetrical methyl transfers.
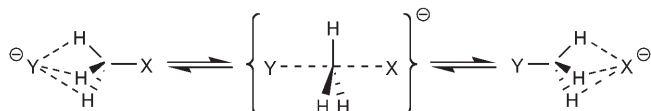
In previous applications of the ISM, it was argued that m accounts for the resonance in the transition state because maximising its electron density is equivalent to maximising its binding energy, and this has the same nature as the traditional resonance between equivalent valence-bond structures of a molecule. The implication of this argument is that the electronic stabilisation owing to the increase of m from unity to the value given by Equation (7) should be comparable to the resonance energy of the VB model of Shaik and Pross, which is expressed by B in Equation (1). Indeed, for symmetrical methyl transfers, in which X = F, Cl, Br and I, B = 29.2, 21.2, 21.1 and 20.2 kcal mol^{-1}, respectively,[19] whereas the energy stabilisations given by Equation (7), when m increases from unity to the value given by Equation (8), are 23.6, 28.8, 27.9 and 27.5 kcal mol^{-1}. Both models predict a similar trend in stabilisation energies when X = Cl, Br and I. However, the VB model predicts a higher stabilisation energy when X = F, whereas the ISM predicts a lower value. As discussed below, with the ISM, part of the stabilisation energy in this latter case is assigned to hydrogen bonding.

Results and Discussion

Symmetrical methyl transfers in the gas phase: It is convenient to start by studying methyl transfers in the gas phase and to avoid solvent effects. However, there is a price to be paid for this simplification. In the gas phase these reactions proceed through the barrierless formation of a precursor ion–dipole complex, followed by the actual methyl transfer and the formation of a successor ion–dipole complex before the final products separate [Mechanism (V)].

$$\text{Y}^- + \text{CH}_3\text{X} \underset{k_{-a}}{\overset{k_a}{\rightleftharpoons}} \{\text{Y} \cdots \text{CH}_3\text{X}\} \overset{k}{\rightarrow} \{\text{YCH}_3 \cdots \text{X}^-\}$$

$$\underset{k_{-d}}{\overset{k_d}{\rightleftharpoons}} \text{YCH}_3 + \text{X}^- \qquad \text{(V)}$$

The structures that are generally believed to represent the complexes and the transition state are presented in Scheme 1 and account for the inversion of configuration in pure SN2 reactions.

Scheme 1. Precursor complex, transition state and successor complex in gas-phase methyl transfer.

It is tempting to draw an analogy between this mechanism and that of proton transfers in the gas phase, which also proceed through the formation of precursor and successor complexes separated by a central barrier.[45] For proton transfers, we have shown that the covalency of the hydrogen bond leads to an incipient proton transfer and reduces the central

barrier. However, the complexes involved in methyl transfers are electrostatic in nature and cannot contribute to the advancement of the bond-breaking–bond-making process. Therefore, the barrier given by Equation (7) should be directly comparable to the central barrier calculated by ab initio methods.

Figure 2 compares the energy barriers calculated with Equation (7) by using $a' = 0.182$ with the central barrier of G2(+) and W1 ab initio calculations.[26,27] These ab initio
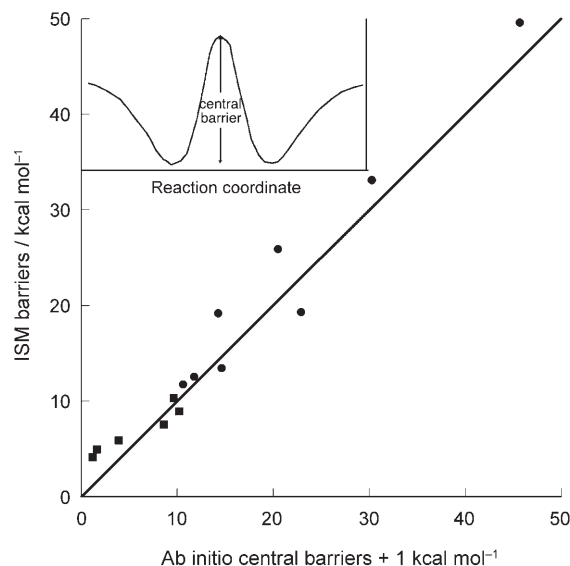

Figure 2. Correlation between the central barriers of gas-phase methyl transfers as determined by ab initio and ISM calculations. ●) Identity transfers of the type: X$^-$ + CH$_3$X (X = CH$_3$CH$_2$, CH$_3$NH, CH$_3$O, F, CH$_3$S, Cl, Br, I).[26,27] ■) Cross-reactions of halide ions with halomethanes.[26,46] The line is the ideal correlation. See the Supporting Information for details.

methods effectively incorporate zero-point vibrational energy (ZPE) corrections, which are absent at this level of ISM calculations. The comparison between ab initio calculations of SN2 reactions between halide ions and halomethanes with and without ZPE corrections reveals that ZPE correction reduces the classical barriers by around 1 kcal mol^{-1}.[23,26,27] Thus, in Figure 2 we added 1 kcal mol^{-1} to the ZPE-corrected ab initio barrier so that we could compare it with the classical ISM barrier. Although the scaling of the ISM was carried out with structural rather than energetic data, it also leads to barriers in good agreement with those of ab initio calculations when harmonic oscillators are employed. The barriers of the CH$_3$O$^-$ + CH$_3$OCH$_3$ and F$^-$ + CH$_3$F systems are overestimated. There is strong evidence that hydrogen bonds are formed between oxygen-centred acids and carbon bases.[47] The precursor complexes of SN2 reactions in the gas phase typically have the structure illustrated in Scheme 1, but when X = F$^-$ or CH$_3$O$^-$ there is significant X···HC bonding in the gas phase[48] and this may contribute to the progress along the reaction coordinate. In proton transfers, we have shown that when hydrogen bond-

ing occurs along the reactions coordinate, it can be regarded as an incipient proton transfer and it reduces the reaction barrier.[45] The reasoning can be extended to the systems mentioned above and the inclusion of hydrogen bonding along the reaction coordinate would bring the calculated barriers into better agreement with those of ab initio calculations. However, rather than introducing a higher degree of sophistication into our calculations, we find it more interesting to explore the relationship between molecular structure and chemical reactivity that they offer.

The ISM calculations reproduce the trends of the ab initio barriers: the central barriers change modestly down the last column and dramatically along the second row of the Periodic Table. The relative constancy of the central barrier within a column of the Periodic Table has a simple explanation within the framework of the ISM. As the atomic number of the halogen atoms increases, the X−C bond lengths increase (1.382, 1.785, 1.933, 2.132 Å), the corresponding force constants decrease (704, 416, 340, 271 kcal mol^{-1} Å^{-2}) and the electrophilicity indices remain approximately constant (1.493, 1.773, 1.796, 1.828). Equation (7) shows that, for a constant m, the decrease in f_{XC} is compensated by the increase in l_{XC} and the barriers remain approximately constant.[29] This compensation is illustrated in Figure 3a.

The ISM also accommodates the decrease in the central barrier along the second row of the Periodic Table. In this case the decrease in l_{XC} (1.532, 1.455, 1.416, 1.382 Å) is not accompanied by a systematic trend in the corresponding force constants (585, 662, 732, 704 kcal mol^{-1} Å^{-2}) and the relative reactivity is dominated by the increase in m (0.938, 1.161, 1.343, 1.493). Figure 3b offers a simple view of the effect of m on the energy barrier, by dividing f_{XC} by m^2. It should always be remembered that this is only a schematic view because the force constants near the minima are given by the spectroscopic properties of the bonds, whereas the full effect of m is only manifested in the transition state.

The beauty of this explanation undoubtedly lies in its straightforwardness and simplicity. Moreover, similar trends have been calculated for the transfer of the $N(CH_3)_2$ group,[49] and confirmed by other authors,[20] in support of the reactivity factors described above.

Symmetrical methyl transfers in solution: The mechanistic complexity of S_N2 reactions is removed in aqueous solutions. In polar solvents, the ionic nature of the reactants and products facilitates their solvation to a higher degree than the precursor or successor complexes. As a result, in a sufficiently polar solvent these complexes disappear from the reaction coordinate and methyl transfer becomes an elementary reaction. For identity transfers, in which $\Delta V^\ominus = 0$, the changes in solvation energy are relatively independent of the nature of the reactants and the trends in reactivity observed for gas-phase reactions can be expected to be observed in solution. The recognition of the same reactivity patterns in symmetrical methyl transfers in the gas phase and in solution suggests that the explanation offered by the
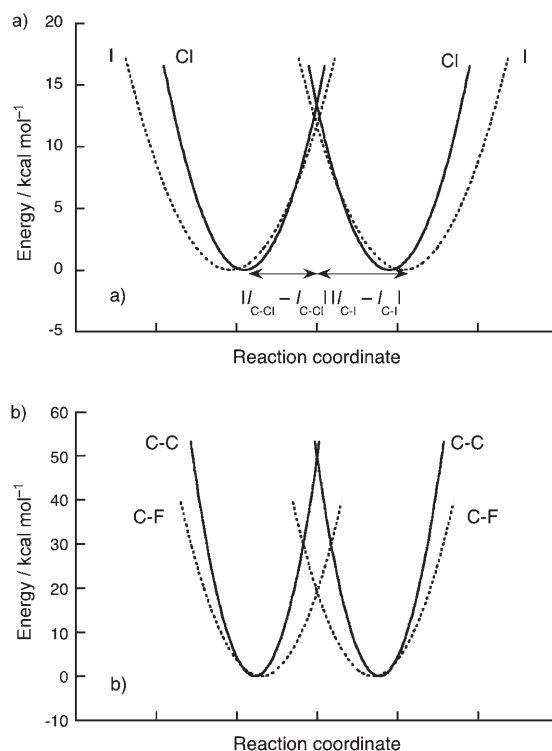

Figure 3. Classical potential-energy dependence on the bond extensions of reactant and product C−X bonds, from their equilibrium to transition-state configurations. The minima are separated by the sum of the bond extensions, $d = |l_{XC}^{\ddagger} - l_{XC}| + |l_{XC}^{\ddagger} - l_{XC}|$. a) Compensation for decreases in force constants and increases in bond lengths. b) Effect of the electrophilicity index m on the transition-state energy, schematically represented by the division of the force constant by m^2.

ISM for such patterns in the gas phase is also applicable to solution. However, the electronic parameter of the ISM, m in Equation (8), is calculated from gas-phase ionisation energies and electron affinities. Before applying the ISM to reactions in solution, it is important to anticipate the changes that can be expected for m.

According to Contreras and co-workers,[50] continuum solvent effects tend to attenuate the electrophilicity index of charged and ionic electrophiles. Thus, on going from the gas phase to a polar solvent, m tends to decrease. Although this qualitative solvent dependence is simple to understand, the actual extent of the decrease in m with the increase in solvent polarity is very difficult to anticipate. Rather than attempting to model solvent properties and correlate them with m, we followed the correlations exposed by Parker et al., which relate solvent effects in S_N2 reaction rates to the corresponding transfer free energy of activation or, empirically, to the solvent acceptor number (AN).[51] The acceptor number measures the ability of solvents to interact with electron pairs from suitable donors. The precise nature of the donor–acceptor interaction (hydrogen bonding, ion–dipole interaction, formation of an acid–base adduct, covalent bonding, etc.) does not need to be specified. A simple functional dependence is given by Equation (9), in which m

is the gas-phase value (AN=0) given by Equation (8) and δ is a sensitivity parameter.

$$m' = m\exp[-\delta \mathrm{AN}] \qquad (9)$$

Figure 4 shows that $\delta = 0.004$ fits very well the values of m' that reproduce the activation energies of *I$^-$+CH$_3$I exchange in water, ethylene glycol, methanol, ethanol and acetone[52] and the G2(+) central barrier in the gas phase with 1 kcal mol^{-1} added to account for the ZPE correction.[27]
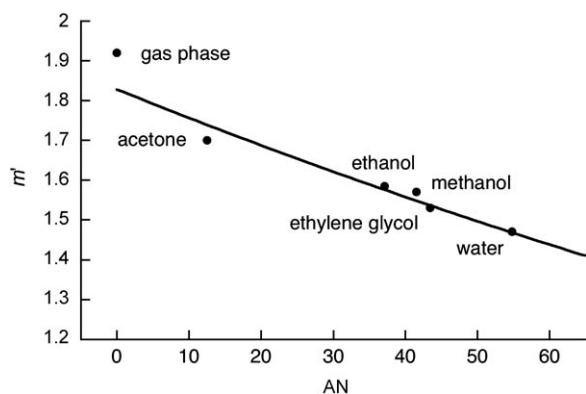

Figure 4. Dependence of the electrophilicity factor on solvent acceptor numbers. The circles represent the values of m' that reproduce the Arrhenius activation energy of the *I$^-$+CH$_3$I exchanges in solution and the classical central barrier in the gas phase. The line was calculated with Equation (10) using $\delta = 0.004$. See the Supporting Information for details.

The Arrhenius activation energies measured in solution differ from the potential-energy barriers calculated with Equation (7). Under the conditions in which the vibrational partition functions are approximately unity, their relation is given by Equation (10),[53] in which $\Delta V_{\mathrm{ad}}^{\ddagger} = \Delta V^{\ddagger} + \mathrm{ZPE}$.

$$E_a = \Delta V_{\mathrm{ad}}^{\ddagger} - RT \qquad (10)$$

The ZPE and RT corrections contribute to a decrease in the reaction barrier of an amount that corresponds to a factor of ten in the rate at room temperature. This can be accommodated in the pre-exponential factor for S$_N$2 reactions and, together with the typical collision factor in solution of $10^{11}\,\mathrm{M^{-1}\,s^{-1}}$, gives $A_0 \approx 10^{10}\,\mathrm{M^{-1}\,s^{-1}}$. Neglecting symmetry factors and tunnelling corrections, the classical ISM/TST rates for S$_N$2 reactions can then be expressed by Equation (11),[31] in which $p = 0,2,3$ when the nucleophile is an atom, a diatomic or a polyatomic species, q_v and q_r are vibrational and rotational partition functions and $(q_v/q_r) \approx 1/3$ and $A_0 \approx 10^{10}\,\mathrm{M^{-1}\,s^{-1}}$. Marcus arrived at essentially the same formulation for polyatomic species from a different approach [see Eq. (20) of ref. [13]].

$$k = A_0 \left(\frac{q_v}{q_r}\right)^p \exp\left(-\frac{\Delta V^{\ddagger}}{RT}\right) \qquad (11)$$

Figure 5 compares the rate constants calculated for *I$^-$+ CH$_3$I exchange with the experimental data obtained in several solvents. The calculated rates are in very good agree-
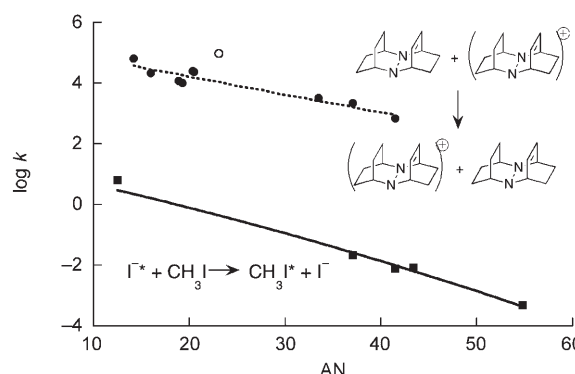

Figure 5. Dependence of the rate constants of the S$_N$2 and electron exchanges indicated in the plot, and the acceptor number of the solvent. ■) The experimental rates of methyl self-exchange and ●) the experimental rates of electron self-exchange.[52, 54] The full line represents the ISM calculated rates. ○ The experimental rate measured in chloroform. It is not included in the electron self-exchange linear correlation (dashed line) because this datum is an outlier in all the correlations with solvent parameters tested.[54]

ment with experimental results, but this agreement benefits from the calibration of Equation (9) with the data in Figure 4. The usefulness of this calibration depends on its generality and this requires the use of cross-reactions.

Methyl cross-reactions in the gas phase: The reaction energy of a cross-reaction in the gas phase can be obtained from the difference in bond dissociation energies and electron affinities of the two reaction partners [Eq. (12)].

$$\Delta H_r^{\ominus} = D_e(\mathrm{C-Br}) - D_e(\mathrm{C-Cl}) + E_A(\mathrm{Cl}) - E_A(\mathrm{Br})$$
$$= -6.0\,\mathrm{kcal\,mol^{-1}} \qquad (12)$$

However, this is not a directly relevant reaction energy for the central barrier of a methyl exchange because the energetic separation between the minima of the precursor and successor complexes may not correspond to the energetic separation between isolated reactants and products. For the reaction illustrated above, the complexation energies for Cl$^-$···CH$_3$Br and Br$^-$···CH$_3$Cl are -12.5 and -10.9 kcal mol^{-1}, respectively,[55] and the energetic separation between the complexes is only 1.6 kcal mol^{-1} less exothermic than $\Delta H_r^{\ominus}$. When the difference between the complexation energies is small, as in the case of alkyl halide···halide ions,[55,56] it is legitimate to expect that the global free energy of the reaction is reflected by the central barrier and that the reactivity follows a free-energy relationship. This is approximately the case for the cross-reactions between halide ions, such as Cl$^-$/CH$_3$Br, F$^-$/CH$_3$Cl and F$^-$/CH$_3$Br, for which the reaction exothermicity, calculated as the energy difference

between separated products and reactants, increases from -6.0 to -35.6 to -41.6 kcal mol^{-1}. According to the ab initio W1 method, the corresponding central barriers are 8.6, 2.9 and 0.7 kcal mol^{-1}.[26] Apparently, this method tends to underestimate these barriers because the experimental barrier for the Cl$^-$/CH$_3$Br exchange is 10.7 kcal mol^{-1}[55] and for the F$^-$/CH$_3$Cl exchange it lies between 5.8 and 8.1 kcal mol^{-1}.[57]

The central barrier of a cross-reaction is determined by the energy of the crossing between reactant and product potential energy curves, as given by Equation (13), in which $\Delta V^\ominus$ is the reaction energy. When the reactant C$-$X and the product C$-$Y bonds are represented by harmonic oscillators, we have Equations (14) and (15), in which the value of n that satisfies the equality of Equation (13) is the transition-state bond order, n^+. As a first approximation, the electronic parameter of the cross-reaction, m_{YX}, can be taken as the average of the values of m for the identity reactions, $m_{YX} = (m_{XX} + m_{YY})/2$. Equations (13) and (14) can be solved iteratively or through the internet site dedicated to ISM calculations.[58] The calculations carried out by using this harmonic approximation and the global reaction energy are in good agreement with the experimental cross-reaction barriers between halide ions, which gave 9.8, 5.1 and 4.5 kcal mol^{-1} for the Cl$^-$/CH$_3$Br, F$^-$/CH$_3$Cl and F$^-$/CH$_3$Br exchanges, respectively. Figure 2 also includes a comparison between cross-reaction rates of halide ions with halomethanes calculated by the ISM and ab initio methods. In addition to the exchanges calculated by the W1 method,[26] Figure 2 also includes the F$^-$/CH$_3$I, Cl$^-$/CH$_3$I and Br$^-$/CH$_3$I exchanges calculated by the G2(+) method.[46]

$$V_{CX}(1-n) = V_{CY}(n) + \Delta V^\ominus \tag{13}$$

$$V_{CX}(1-n) = \frac{1}{2} f_{CX} \left[\frac{a'(l_{CX} + l_{CY}) \ln(1-n)}{m_{YX}} \right]^2 \tag{14}$$

$$V_{CY}(n) = \frac{1}{2} f_{CY} \left[\frac{a'(l_{CX} + l_{CY}) \ln(n)}{m_{YX}} \right]^2 \tag{15}$$

It is well known that gas-phase S$_N$2 cross-reactions of halide ions with halomethane ions follow a linear free-energy relationship, namely the Bell–Evans–Polanyi relationship,[59,60] $\Delta V^+_{ad} = \alpha \Delta V^\ominus_{ad} + V^\ominus_{ad}$, in which α is a constant and $V^\ominus_{ad}$ an intrinsic barrier. However, the success of this approach to the analysis of gas-phase methyl transfers is limited by the difference in the stabilisation energies of the precursor and successor complexes. For example, the overall F$^-$ + CH$_3$SH methyl transfer is exothermic, $\Delta H^\ominus_r = -11.5$ kcal mol^{-1}, but the central barrier is placed between two minima corresponding to ion–molecule complexes whose endothermic conversion requires $\Delta V^\ominus_{ad} = 18.0$ kcal mol^{-1}.[25] Although the reaction energy, measured for the separated products from the separated reactants, is moderately exothermic, the actual reaction involves a precursor and a successor complex that must be regarded as reaction intermediates. The conversion between these two intermediates is an elementary reaction and is endothermic because

the electrostatic stabilisation in the F$^-$ + CH$_3$SH complex is stronger than in the HS$^-$ + CH$_3$F complex. The barrier calculated for the elementary reaction is high, $\Delta V^+_{ad} = 39.6$ kcal mol^{-1},[25] as expected for an endothermic reaction, but the energy of the transition state is only 1.6 kcal mol^{-1} above that of the separated reactants. According to the ISM, when $\Delta V^\ominus = 18.0$ kcal mol^{-1}, $\Delta V^+ = 28.3$ kcal mol^{-1}.

This example shows that free-energy relationships can only be applied to elementary reactions otherwise they will fail or fortuitously give the correct results as a result of compensation of factors. Moreover, the presence of a stable intermediate may reduce the experimental activation energy and may even lead to a negative energy of activation. In such cases, the treatment of the reaction rates by using classical transition-state theory is not recommended. These limitations are not present for S$_N$2 cross-reactions in solution.

Methyl cross-reactions in solution: A first rationale for the activation free energies of methyl transfer cross-reactions in solution was presented by Albery and Kreevoy[61] in terms of the Marcus cross-relation given by Equation (16), in electrostatic which work terms were neglected. The reorganisation energy, λ, is related to the average of the free energies of activation for the symmetrical reactions, $\lambda = 4(\Delta G^+_{XX} + \Delta G^+_{YY})/2$. This rationale met with considerable success in explaining the free-energy dependence of methyl transfers.

$$\Delta G^+_{XY} = \frac{\lambda}{4} \left(1 + \frac{\Delta G^\ominus_{XY}}{4\lambda} \right)^2 \tag{16}$$

Note that Albery and Kreevoy expressed the cross-relation in terms of free energies and this leads to a systematic difference compared with the experimental activation energies. Empirically, $\Delta G^+ \approx E_a + 3.5$ kcal mol^{-1} when the pre-exponential factors in solution are $A_0 \approx 10^{10}$ M^{-1}s^{-1}. The entropy changes along the reaction path of the Cl$^-$ + CH$_3$Cl reaction have been calculated with high accuracy by ab initio methods[21] and allow a comparison between ΔG^+ and E_a. The central free-energy barrier given by the sum of the ZPE-corrected central barrier (G3 method: 13.0 kcal mol^{-1}) and the entropy change for the formation of the transition state from the ion–dipole complex (DFT method: -8.7 e.u. at 300 K) is $\Delta G^+ = 15.6$ kcal mol^{-1}.[21] According to these calculations, the central free-energy barrier is 2.6 kcal mol^{-1} higher than the corresponding potential-energy barrier, which supports the empirical estimate.

Figure 6 compares the experimental rate constants obtained at 25°C in water[62,63] with the rate constants calculated with Equation (11) by using $\Delta V^\ominus \approx \Delta G^\ominus$; the reaction energies were taken from the work of Albery and Kreevoy[61] or from the ratio of the forward and reverse reactions.[62,63] The bond lengths and force constants presented in Table 1 and the value of m' given by Equation (9) with $\delta = 0.004$ were used to calculate the ISM/TST rates in solution. Except for the OH$^-$ + CH$_3$F reaction, which is 45 times faster than the calculated rate, the agreement between calculated and experimental rates is very good. The discrepan-
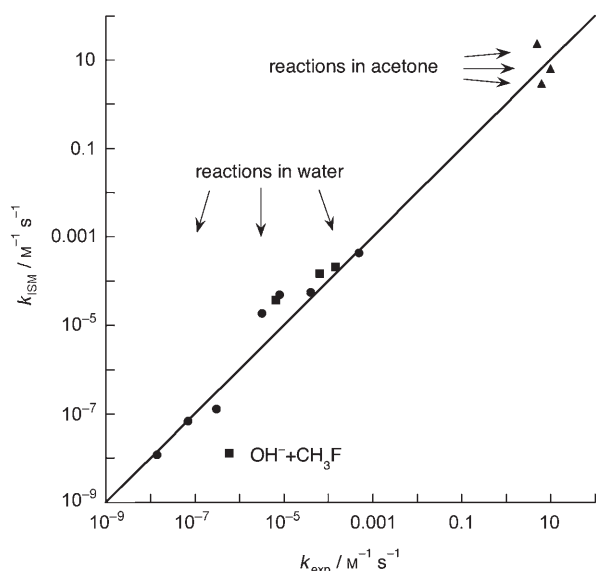
Figure 6. Comparison between the ISM and experimental methyl transfer rate constants in water (■ and ●)[62,63] and acetone (▲)[52,63] at 298 K. ●) X$^-$+CH$_3$X; ■) OH$^-$+CH$_3$X. In all cases, X = F, Cl, Br, I. See the Supporting Information for details.

cy observed for the OH$^-$+CH$_3$F reaction may be related to the fact that the rates were experimentally measured in the 80–120 °C temperature range and extrapolated to 25 °C,[64] in contrast with the alkaline hydrolysis of the other methyl halides, which were measured in the 20–70 °C temperature range.[65]

More interesting than reproducing the precise rate constants of methyl transfer in solution is to gain some understanding of the extraordinary solvent dependence of these rates. For example, the rate constant for the Cl$^-$+CH$_3$I methyl exchange increases from 3.2×10^{-6} M^{-1}s^{-1} in water to 5.1 M^{-1}s^{-1} in acetone.[63] We calculate $\Delta G^\ominus = 1.1$ kcal mol^{-1} from the forward and reverse reaction rates in water and $\Delta G^\ominus = -4.9$ kcal mol^{-1} from the equilibrium constant in acetone.[62] With these reaction free energies we obtain $k_{ISM} = 1.9 \times 10^{-5}$ M^{-1}s^{-1} in water and 24 M^{-1}s^{-1} in acetone. Thus, the calculations reproduce the more than six orders of magnitude increase in the rate when the solvent is changed from water to acetone. Changing the reaction free energy with the solvent without changing m' leads to only a two-fold increase in the rate. The increase in m' from 1.446 in water to 1.712 in acetone contributes to a rate enhancement of four orders of magnitude. This is also the rate enhancement observed and calculated for *I$^-$+CH$_3$I exchange in Figure 5, in which $\Delta G^\ominus = 0$.

A similar example is the Br$^-$+CH$_3$I methyl exchange, whose rate constant increases from 4.0×10^{-5} M^{-1}s^{-1} in water[63] to 10 M^{-1}s^{-1} in acetone, whereas $\Delta G^\ominus$ changes from 1.2 to -1.9 kcal mol^{-1}, according to the respective ratios of the forward and reverse rates.[63] We calculate that k_{ISM} increases from 5.5×10^{-5} to 6.5 M^{-1}s^{-1} with this change in solvent. The experimental and calculated rate increases are now smaller than those for the Cl$^-$+CH$_3$I exchange and ac-

count for the reversal in the order of nucleophilicity: Br$^-$ is a better nucleophile than Cl$^-$ in water, but not in acetone. This reversal can be assigned to the change in the thermodynamic driving force of these reactions with solvent because the symmetrical exchange in the gas phase involving Br$^-$ has a slightly lower barrier than that involving Cl$^-$.[26]

To rationalise the success of the ISM in calculating the rates of methyl transfer in different solvents with the same sensitivity parameter, $\delta = 0.004$, we substitute Equation (9) into Equation (7), retain only the first two terms in the infinite series that defines the exponential function and express the rate of a symmetrical reaction in a solvent s with respect to a reference solvent 0 as Equation (17), in which b is a constant related to the force constant, bond length and electrophilicity index. This equation is analogous to the empirical dependence of $\Delta G^\ddagger_{tr}$ on $\Delta(AN)$ found by Parker et al.[51] However, they found that the slope of $\Delta G^\ddagger_{tr}$ versus $\Delta(AN)$ depended on the nature of the reactants. This restriction is raised by the present ISM calculations because we have taken into account the nature of the reactants and the reaction energy in each solvent.

$$\Delta G^\ddagger_{tr} = -RT\ln\left(\frac{k_s}{k_0}\right) = -b\delta(AN_s - AN_0) = b\delta\Delta(AN) \quad (17)$$

The conventional view of solvent effects in S$_N$2 reactions dramatises the importance of anion solvation.[4] The nature of the solvent effect revealed by the ISM is the use of the anion solvating power of the solvent to delocalise the electrons of the nucleophile to regions away from the reaction coordinate. In fact, the acceptor number expresses the ability of the solvent to accept an electron-pair from the nucleophile. When AN is high, the electron inflow at the transition state saturates at a lower point because part of the electron density of the nucleophile is coupled to the solvent and the value of m is lower. The result is less resonance in solvents with high AN and a higher energy barrier. This is a static solvent effect and, together with the thermodynamic effect of the solvent in the reaction energy, appears to dominate solvent effects in S$_N$2 reactions.

S$_N$2 versus electron-transfer mechanisms: An important distinction between S$_N$2 and outer-sphere ET mechanisms is the degree of resonance in the transition state. As discussed above, methyl exchanges of halide ions with halomethanes have resonance energies of between 20 and 30 kcal mol^{-1} and are associated with transition-state bond lengths of between 1.8 and 2.7 Å. Outer-sphere ET reactions are usually believed to have resonance energies of less than 1 kcal mol^{-1} in solution and to be structureless.[66] However, diatomic ion–molecule ET exchanges in the gas phase also involve the formation of precursor and successor complexes with significant electronic couplings between the two reactants. For example, Ohta and Morokuma calculated an electronic coupling of 13.4 kcal mol^{-1} for O$_2$/O$_2^-$ exchange, with the parallel axis formed by the two sets of nuclei 3.18 Å apart, and argued that an adiabatic approach with a proper transi-

tion state should be preferred over the non-adiabatic, radiationless-transition approach.[67] Similar bonding was found in the ET transition state of the $NCCHO^{\cdot-} + CH_3Cl$ reaction, with a coupling of more than 14 kcal mol^{-1}, when the C—C bond length in the transition state is 2.4 Å.[15] In this and related reactions the same transition state has been shown to serve both S_N2 and ET mechanisms.[14,16] These examples of ET transition states come close to meeting the criteria for inner-sphere ET, which should have transition-state resonance interactions of between 7 and 2.3 kcal mol^{-1} and distances between the two reactant moieties ranging from 3.0 to 3.5 Å.[11]

The change from S_N2 to ET character is heightened when active orbitals are highly encumbered sterically. Steric effects in S_N2 reactions increase the reaction barriers. For example, the barriers for the reactions of Br$^-$ with methyl, ethyl, isopropyl and tert-butyl bromides in acetone increase by 2 kcal mol^{-1} for each replacement of a hydrogen atom by a methyl group.[68] Ab initio calculations support the view that steric effects are similar in the gas phase and in solution.[69] The increase in the reaction barriers owing to the longer transition-state bond lengths imposed by steric effects can be accommodated by our model by using a higher value of a'. By using the data obtained from the Br$^-$ + CH$_3$Br reaction in acetone and increasing a' from 0.182 to 0.218 by 0.012 every time a hydrogen atom is replaced by a CH$_3$ group, reproduces the 2 kcal mol^{-1} increases experimentally observed. Similar calculations for the methyl and ethyl exchanges in Cl$^-$ + CH$_3$Cl and Cl$^-$ + CH$_3$CH$_2$Cl gave nearly identical energetic results and an increase of 0.03 Å in the transition-state bond lengths, similar to the 0.04 Å increase in C—Cl distance obtained by other semiempirical methods.[69] This naive treatment of steric effects serves to illustrate that a' may have to be scaled to different reference systems when a different class of reaction is studied. Nevertheless, it is quite evident that when active orbitals are centred in atoms more than 4 Å apart, the S_N2 mechanism becomes inoperative.

As the distance between the orbitals in the reactive complex becomes larger, their overlap becomes smaller. When the distance exceeds 6 Å, the resonance energy drops below 1 kcal mol^{-1}[11] and the reaction becomes truly non-adiabatic. In non-adiabatic reactions, such as outer-sphere ET, the separation between the reactants does not affect the reaction barrier. Rather, it is the pre-exponential factor that decreases exponentially with the separation between the reactants. The electron exchange between alkylhydrazines and their radical cations is a good example of an outer-sphere ET in the gas phase because the sphere centred on the N—N bonds of typical alkylhydrazines has a radius of around 4 Å.[70] The solvent dependence of these reactions is illustrated in Figure 5.[54] The weak solvent dependence of the self-exchanges, the similar barriers in the gas phase and in acetonitrile and the constancy of the barrier for reactants of very different sizes led Nelsen et al. to conclude that the contribution of the solvent to the barrier is always less than 2 kcal mol^{-1} and the primary factor governing ET reactivity is the

structural reorganisation.[71] The same conclusion had been reached in the ISM studies of these reactions.[72] It must be emphasised that in the ISM calculations of outer-sphere ET self-exchange rates, the parameter m in Equation (7) is replaced by $2n_0$, in which n_0 is the bond order of the reactive bond, because the integrity of the bonds is preserved in these reactions and their transition-state resonance is small.[72,73] Also, the value of a' is smaller and identical to that used to reproduce the activation energies of hydrogen-atom abstractions by radicals, $a' = 0.156$,[31,74] as expected from the small steric effects and electronic repulsion in these reactions.

Bimolecular ET reactions are favoured over methyl transfers by their lower a', higher pre-exponential factor and $2n_0/m' > 1$. However, the large CH$_3$—X bond dissociation energy makes the thermodynamics of the ET reaction in Mechanism (3) very unfavourable and unable to compete efficiently with the methyl transfer of Mechanism (1). For systems with smaller bond dissociation energies and low resonances ($m \approx 1$), ET can effectively compete with S_N2 and this should be gauged by the loss of stereospecificity of the reactions. The competition between S_N2 and ET mechanisms reflects the evolution of the system along different reaction coordinates. The methyl transfer reaction coordinate is characterised by the conservation of the total bond order and by a large resonance energy in the transition state. A typical outer-sphere ET may occur between reactants at large separations, with small resonance energy and uncorrelated bond order changes within each reactant. Each of these reaction coordinates can be treated independently of each other with appropriate models.

Conclusion

The very simple model presented here for S_N2 reactions gives a consistent view of methyl transfers, with proper transition-state structures, clear relationships between molecular structure and reactivity, and a rationale for their solvent dependence. The model requires information on only the bond lengths, force constants, ionisation potentials and electronic affinities of the reactants to calculate their intrinsic barriers in the gas phase. A simple empirical extension to calculate the rate constants in solution requires only one solvent parameter (its acceptor number), in addition to the thermodynamics of the reaction in that solvent.

The resonance in the transition state plays an important role in its stabilisation with consequent implications for the height of the reaction barrier. Although this resonance was assessed mostly by using information on the unidimensional reaction coordinate of the ISM, for reactions in solution this is not sufficient. Solvents with larger acceptor numbers interact strongly with the reactants and remove part of the electron density away from the ISM reaction coordinate, which leads to increased barriers. The classical argument for the slowness of S_N2 reactions by ionic nucleophiles in polar solvents is that the accentuated dispersal of the charge on

the transition state leads to a poorer solvation of the transition state compared with the reactants. The ISM and classical interpretations are clearly related, as the removal of the electron density measured by the acceptor number is also a measure of the dispersal of charge. However, the ISM offers a quantitative approach to this effect, which is transferable between nucleophiles and solvents.

The $H^- + CH_3H$ exchange, ignored so far, is a less obvious case for which the unidimensional reaction coordinate of the ISM is not enough to describe the reactivity. The electron density in the transition state of this exchange process is delocalised away from the $H\cdots C\cdots H$ reaction coordinate because there are three additional C—H bonds identical to the two selected for the reaction coordinate. This was presented in the VB theory of Shaik, Pross and co-workers by a larger f factor.[17,75,76] Alternatively, this effect can be regarded as giving rise to a transition-state bond order of less than 0.5 for this symmetrical reaction. A lower n^+ value leads to longer extensions of the reactive bonds in Equation (4), and a higher barrier in Equation (7). Indeed, VB calculations show that the odd-electron density on the carbon in the active bond is 0.29.[75] We can estimate n^+ by adding the contribution to the bond order of the departing electron in the active orbital of the nucleophile, $n_{XC} = 0.5$, that of the electron in the active bond of carbon, $n_{YC} < 0.29$, to obtain $n^+ = (n_{XC} + n_{YC})/2 < 0.395$. This upper limit for n^+, together with $f_{CH} = 720$ kcal mol^{-1} Å^{-2} from the CH$_4$ bonds and $m = 1.117$ from the electronic data of the hydrogen atom, gives a barrier of $\Delta V^+ > 39$ kcal mol^{-1} with Equation (7), which is consistent with the ab initio barrier of 51.2 kcal mol^{-1} measured from the well of the reactant complexes.[23] Further evidence for our interpretation can be found in the ab initio calculations of Lee et al., who found a C—H bond length extension of 50%, which is much longer than the percentage bond extensions of the systems presented in Figure 1 that are around 30%.[23] This interpretation is further corroborated by the data on the simplest S$_N$2 reaction, $H^- + H_2$, for which there is no ambiguity of the reaction coordinate. With $n^+ = 0.5$, we calculate a barrier of 11.5 kcal mol^{-1}, which is nearly identical to the ab initio barrier measured from the van der Waals minimum, 11.9 kcal mol^{-1}.[42] With the same $n^+ = 0.5$, the ab initio and ISM transition-state bond extensions of this system are in good agreement, as illustrated in Figure 1.

Finally, it is interesting to compare the solvent dependence of S$_N$2 and ET reactions. Both involve the transfer of a single electron from the nucleophile to the leaving group. Outer-sphere ET reactions can be further distinguished by a low resonance in the transition state that is independent of the solvent. Considering only ET self-exchanges, in which $\Delta G^\ominus = 0$, the low resonance in apolar solvents cannot be much reduced by polar solvents and static solvent effects should be smaller than for symmetrical methyl transfers. The weak solvent dependence of ET self-exchanges has been experimentally observed and this is the basis for the success of ISM applications to electron transfer.[72]

[1] C. K. Ingold, *Structure and Mechanism in Organic Chemistry*, Cornell University Press, Ithaca, NY, **1969**, p. 427.

[2] L. Arnaut, S. Formosinho, H. Burrows, *Chemical Kinetics*, Elsevier, Amsterdam, **2007**, p. 273.

[3] M. B. Smith, J. March, *March's Advanced Organic Chemistry*, Wiley, New York, **2001**, p. 432.

[4] T. H. Lowry, K. S. Richardson, *Mechanism and Theory in Organic Chemistry*, Harper & Row, New York, **1987**, p. 353.

[5] A. Pross, S. Shaik, *J. Am. Chem. Soc.* **1981**, *103*, 3701–3709.

[6] A. Pross, S. Shaik, *Acc. Chem. Res.* **1983**, *16*, 363–370.

[7] J.-M. Savéant, *Adv. Phys. Org. Chem.* **1990**, *26*, 1–130.

[8] A. Pross, *Adv. Phys. Org. Chem.* **1985**, *21*, 99–196.

[9] H. Lund, K. Daasbjerg, T. Lund, S. U. Pedersen, *Acc. Chem. Res.* **1995**, *28*, 313–319.

[10] Y.-M. Xing, X.-F. Xu, L. Chen, Z.-S. Cai, X.-Z. Zhao, J.-P. Cheng, *Phys. Chem. Chem. Phys.* **2002**, *4*, 4669–4677.

[11] L. Eberson, S. S. Shaik, *J. Am. Chem. Soc.* **1990**, *112*, 4484–4489.

[12] J.-M. Savéant, *J. Am. Chem. Soc.* **1992**, *114*, 10595–10602.

[13] R. A. Marcus, *J. Phys. Chem. A* **1997**, *101*, 4072–4087.

[14] J. Li, X. Li, S. Shaik, H. B. Schlegel, *J. Phys. Chem. A* **2004**, *108*, 8526–8532.

[15] V. Bakken, D. Danovich, S. Shaik, H. B. Schlegel, *J. Am. Chem. Soc.* **2001**, *123*, 130–134.

[16] H. Yamataka, M. Aida, M. Dupuis, *J. Phys. Org. Chem.* **2003**, *16*, 475–483.

[17] S. S. Shaik, A. Pross, *J. Am. Chem. Soc.* **1982**, *104*, 2708–2719.

[18] S. S. Shaik, *Prog. Phys. Org. Chem.* **1985**, *15*, 197–337.

[19] L. Song, W. Wu, P. C. Hiberty, S. Shaik, *Chem. Eur. J.* **2006**, *12*, 7458–7466.

[20] E. Uggerud, *Chem. Eur. J.* **2006**, *12*, 1127–1136.

[21] S.-Y. Yang, P. Fleurat-Lessard, I. Hristov, T. Ziegler, *J. Phys. Chem. A* **2004**, *108*, 9461–9468.

[22] L. Sun, K. Song, W. L. Hase, *Science* **2002**, *296*, 875–878.

[23] I. Lee, C. K. Kim, C. K. Sohn, H. G. Li, H. W. Lee, *J. Phys. Chem. A* **2002**, *106*, 1081–1087.

[24] G. D. Ruggiero, I. H. Williams, *J. Chem. Soc., Perkin Trans. 2* **2002**, 591–597.

[25] J. M. Gonzales, R. S. Cox III, S. T. Brown, W. D. Allen, H. F. Schaefer III, *J. Phys. Chem. A* **2001**, *105*, 11327–11346.

[26] S. Parthiban, G. De Oliveira, J. M. L. Martin, *J. Phys. Chem. A* **2001**, *105*, 895–904.

[27] S. Hoz, H. Basch, J. L. Wolk, T. Hoz, E. Rozental, *J. Am. Chem. Soc.* **1999**, *121*, 7724–7725.

[28] M. N. Glukhovtsev, A. Pross, L. Radom, *J. Am. Chem. Soc.* **1995**, *117*, 2024–2032.

[29] L. G. Arnaut, A. A. C. C. Pais, S. J. Formosinho, *J. Mol. Struct.* **2001**, *563/564*, 1–17.

[30] Y. Ren, J. L. Wolk, S. Hoz, *Int. J. Mass Spectrom.* **2002**, *220*, 1–10.

[31] L. G. Arnaut, A. A. C. C. Pais, S. J. Formosinho, M. Barroso, *J. Am. Chem. Soc.* **2003**, *125*, 5236–5246.

[32] L. G. Arnaut, S. J. Formosinho, M. Barroso, *J. Mol. Struct.* **2006**, *786*, 207–214.

[33] M. Barroso, L. G. Arnaut, S. J. Formosinho, *J. Phys. Chem. A* **2007**, *111*, 591–602.

[34] H. S. Johnston, C. Parr, *J. Am. Chem. Soc.* **1963**, *85*, 2544–2551.

[35] L. Pauling, *J. Am. Chem. Soc.* **1947**, *69*, 542–553.

[36] *Handbook of Chemistry and Physics*, 3rd electronic edition, CRC Press, Boca Raton, FL (USA), **2001**.

[37] K. Nakamoto, *Infrared Spectra of Inorganic and Coordination Compounds*, Wiley, New York, **1963**, p. 72.

[38] Y.-R. Luo, *Handbook of Bond Dissociation Energies in Organic Compounds*, CRC Press, New York, **2003**.

[39] G. da Silva, C.-H. Kim, J. W. Bozzelli, *J. Phys. Chem. A* **2006**, *110*, 7925–7934.

[40] S. J. Blanksby, G. B. Ellison, *Acc. Chem. Res.* **2003**, *36*, 255–263.

[41] K. Kyllönen, S. Alanko, J. Lohilahti, V.-M. Horneman, *Mol. Phys.* **2004**, *102*, 1597–1604.

[42] A. N. Panda, N. Sathyamurthy, *J. Chem. Phys.* **2004**, *121*, 9343–9351.

[43] A. A. Zavitsas, C. Chatgilialoglu, *J. Am. Chem. Soc.* **1995**, *117*, 10645–10654.

[44] R. G. Parr, L. v. Szentpály, S. Liu, *J. Am. Chem. Soc.* **1999**, *121*, 1922–1924.

[45] M. Barroso, L. G. Arnaut, S. J. Formosinho, *ChemPhysChem* **2005**, *6*, 363–371.

[46] M. N. Glukhovtsev, A. Pross, L. Radom, *J. Am. Chem. Soc.* **1996**, *118*, 6273–6284.

[47] R. Taylor, O. Kennard, *J. Am. Chem. Soc.* **1982**, *104*, 5063–5070.

[48] J. K. Laerdahl, E. Uggerud, *Int. J. Mass Spectrom.* **2002**, *214*, 277–314.

[49] R. Yi, H. Basch, S. Hoz, *J. Org. Chem.* **2002**, *67*, 5891–5895.

[50] P. Pérez, A. Toro-Labbé, R. Contreras, *J. Am. Chem. Soc.* **2001**, *123*, 5527–5531.

[51] A. J. Parker, U. Mayer, R. Schmid, V. Gutmann, *J. Org. Chem.* **1978**, *43*, 1843–1855.

[52] E. R. Swart, L. J. Le Roux, *J. Chem. Soc.* **1957**, 406–410.

[53] S. Glasstone, K. J. Laidler, H. Eyring, *The Theory of Rate Processes*, McGraw Hill, New York, **1941**, p. 195.

[54] S. F. Nelsen, Y. Kim, S. C. Blackstock, *J. Am. Chem. Soc.* **1989**, *111*, 2045–2051.

[55] C. Li, P. Ross, J. E. Szulejko, T. B. McMahon, *J. Am. Chem. Soc.* **1996**, *118*, 9360–9367.

[56] R. C. Dougherty, J. D. Roberts, *Org. Mass Spectrom.* **1974**, *8*, 81–83.

[57] M. J. Pellerite, J. I. Brauman, *J. Am. Chem. Soc.* **1983**, *105*, 2672–2680.

[58] http://www.ism.qui.uc.pt:8180/ism/, ISM_APT, L. G. Arnaut, M. Barroso, D. Oliveira, University of Coimbra, Coimbra, **2006**. Files for S_N2 calculations follow the same format as for proton transfer, with two differences: the first number must be "−2" rather than "1" and an additional number must be included in a new line before the first comment line introducing temperatures and experimental rates. This number is the AN of the solvent.

[59] R. P. Bell, *Proc. R. Soc. London, Ser. A* **1936**, *154*, 414–429.

[60] M. G. Evans, M. Polanyi, *Trans. Faraday Soc.* **1936**, *32*, 1333–1360.

[61] J. Albery, M. M. Kreevoy, *Adv. Phys. Org. Chem.* **1978**, *16*, 87–157.

[62] E. A. Moelwyn-Hughes, *The Chemical Statics and Kinetics of Solutions*, Academic Press, London, **1971**, p. 234.

[63] A. J. Parker, *Chem. Rev.* **1969**, *69*, 1–32.

[64] D. N. Glew, E. A. Moelwyn-Hughes, *Proc. R. Soc. London, Ser. A* **1952**, *211*, 254–264.

[65] E. A. Moelwyn-Hughes, *Proc. R. Soc. London, Ser. A* **1949**, *196*, 540–553.

[66] R. A. Marcus, N. Sutin, *Biochim. Biophys. Acta* **1985**, *811*, 265–322.

[67] K. Ohta, K. Morokuma, *J. Phys. Chem.* **1987**, *91*, 401–406.

[68] P. B. D. de la Mare, *J. Chem. Soc.* **1955**, 3180–3318.

[69] G. Vayner, K. N. Houk, W. L. Jorgensen, J. I. Brauman, *J. Am. Chem. Soc.* **2004**, *126*, 9054–9058.

[70] S. F. Nelsen, D. T. Rumack, M. Meot-Ner (Mautner), *J. Am. Chem. Soc.* **1987**, *109*, 1373–1379.

[71] S. F. Nelsen, M. N. Weaver, J. R. Pladziewicz, L. K. Ausman, T. L. Jentzsch, J. J. O'Konek, *J. Phys. Chem. A* **2006**, *110*, 11665–11676.

[72] S. J. Formosinho, L. G. Arnaut, R. Fausto, *Prog. React. Kinet.* **1998**, *23*, 1–90.

[73] C. Serpa, P. J. S. Gomes, L. G. Arnaut, S. J. Formosinho, J. Pina, J. Seixas de Melo, *Chem. Eur. J.* **2006**, *12*, 5014–5023.

[74] A. J. C. Varandas, S. J. Formosinho, *J. Chem. Soc., Faraday Trans. 2* **1986**, *82*, 953–962.

[75] G. Sini, S. S. Shaik, J.-M. Lefour, G. Ohanessian, P. C. Hiberty, *J. Phys. Chem.* **1989**, *93*, 5661–5665.

[76] S. Shaik, P. C. Hiberty, *Adv. Quantum Chem.* **1995**, *26*, 99–163.